Lidar Design Study for Turbulence Sensing from Ground into the Free Atmosphere Based on Angle-of-Arrival Fluctuation Analysis

P. Vrancken
Institute of Atmospheric Physics, German Aerospace Center (DLR), 82234 Weßling, Germany
Email: patrick.vrancken@dlr.de

Based on explicit, experimentally proven formulae (Zilberman & Kopeika, 2008), an ameliorated lidar scheme for turbulence retrieval over a large range of distances is proposed, with emphasis on state-of-the-art hardware and useful turbulence parameters resolution.

Except for very few exceptions, turbulence sensing by lidar today is based on coherent Doppler wind lidar and thus restricted to the boundary layer (as thoroughly reviewed in (Sathe & Mann, 2013)). This investigated turbulence due to velocity fluctuations is related to temperature fluctuation turbulence. The latter gives rise to fluctuations in the refractive index, commonly termed “optical turbulence” (OT) and quantified by its structure constant C_n^2. OT itself may thus well be used for monitoring and quantifying atmospheric turbulence. One manifestation of OT are angle-of-arrival (AoA) fluctuations (of an imaged laser spot at a certain altitude) and arise as a combination of the following effects: In a vertical pulsed lidar setup, an upward laser beam undergoes deviations from the straight line due to traversing different temperature cells (and thus refractive index jumps), thus shifting the illuminated volume from pulse to pulse (due to advection of the turbulent and temperature cells). On the way down, the 4π-scattered radiation experiences wavefront distortion due to the same refractive index inhomogeneities. As a consequence, the image of the laser beam “spot” (range gate volume) “dances” within the focal plane of the lidar. This shot-to-shot movement, or its envelope, may be quantified for OT and thus general turbulence retrieval.

For a given C_n^2 altitude profile, integrated angle-of-arrival (AoA) fluctuations may be derived with the following relationship, resulting from rigorous treatment of the underlying atmospheric-optics physics (Zilberman & Kopeika, 2008):

$$\langle {\varphi_{AA}}^2 \rangle (L) = \left(\frac{4.07}{{w_0}^{1/3}} + \frac{5.65}{D^{1/3}} \right) \cdot \int_0^L {C_n}^2(z) \cdot \left(1 - \frac{z}{L}\right)^{5/3} dz \quad (1)$$

where w_0 is the lidar’s emitted laser beam radius, D the lidar’s receive telescope diameter, both contributing to a “geometric pre-factor” while $C_n^2(z)$ is the profile over altitude z. Both different $C_n^2(z)$ profiles and related AoA $\sigma_{AA} = \sqrt{\langle {\varphi_{AA}}^2 \rangle}$ fluctuations (standard deviation) are shown in the graphs.

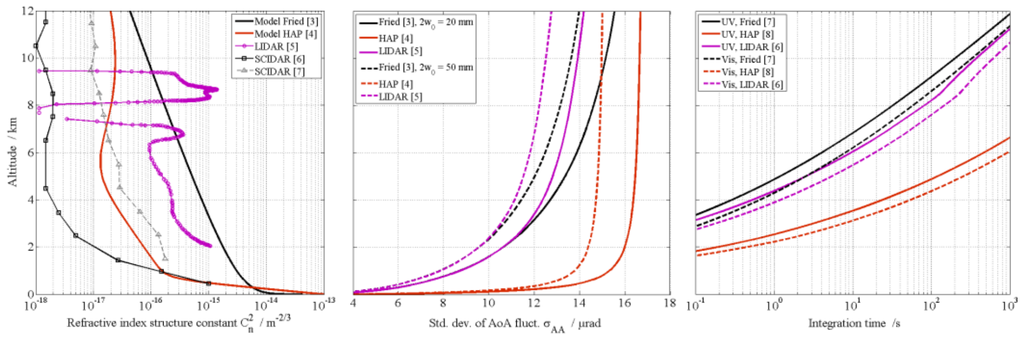

Figure: C_n^2-model profiles by (Fried & Cloud, 1966), upgraded Hufnagel-Valley (Andrews et al., 2012), with actual measurements by AoA-lidar (Zilberman & Kopeika, 2004) and astronomy-site SCIDAR measurements (Liu et al., 2013; Vernin et al., 2009), for illustration. From such C_n^2-profiles, AoA fluctuations are derived (middle panel) for two different laser beam diameters. This leads to necessary integration times for determining turbulence profiles with 100 m vertical resolution based on synthetic *SNR*.

Within the optical assembly, the usable AoA-fluctuation quantity may be sized to arbitrary dimensions for physical observation employing an optical system with $\langle {x_{Det}}^2 \rangle = \langle {\varphi_{AA}}^2 \rangle \cdot f_{\text{eff}}$, where f_{eff} is the effective focal length of an imaging system onto a detector, and x_{Det} the respective position on the detector.

For optimum detection, Equation (1) has to be tuned for maximum possible beam fluctuation, minimum laser beam spread and also maximum photon yield – these criteria behaving oppositely. The pre-factor increases the AoA fluctuation extent when reducing the initial laser beam radius, in turn leading to higher diffractive divergence but less turbulent beam spread, the latter may be calculated by an approach presented by (Andrews & Phillips, 2005).

In the next step, the actually backscattered signal is considered. For calculating the signal within the familiar lidar equation, the sum of molecular and expected aerosol backscatter from a conservative global model, ESA's RMA (Vaughan et al., 1998), is used. Instead of a longer signal integration (i.e. direct summation) onto a two-dimensional detector (like a CCD as in (Zilberman & Kopeika, 2004)), an optical compression along one dimension (by a cylindrical lens) with imaging onto a line detector is proposed. This layout has shown high benefit in a another lidar project (Vrancken & Herbst, 2019). Without considerable loss of information, the 2D image of the integrated "dancing" laser spot is thus transformed into a 1D Gaussian on a multi-element PMT line array. In the following example (with $2w_0$ = 50 mm, C_n^2 Fried model), the detector should span approximately 128 µrad.

Then, for detection performance analysis, the single-shot *SNR* for the single PMT elements is determined. These detector *SNR*s are calculated for an Nd:YAG laser of E_{Vis} = 110 mJ, E_{UV} = 60 mJ (based on a state-of-the-art commercial specimen), a commercial 32 elements PMT array with width-to-pitch ratio of 0.8 and typical lidar parameters and constraints.

The summation of an adequate number N_Σ of these single pulses yields the total AoA fluctuation distribution whose width has to be determined with sufficient resolution R_{AA}.

For a height-resolved analysis an inversion has to be performed. Then, for correctly resolving the gradients of $\langle {\varphi_{AA}}^2 \rangle$ for a needed altitude resolution, a certain synthetic SNR_Σ has to be achieved: For instance, the gradient amounts to 1.8 ‰ over 100 m (Fried model in 9 km altitude) and thus implies an SNR_Σ = 560. Considering a certain laser pulse repetition rate (here 100 Hz) one may readily determine the needed averaging times for a certain aimed altitude and resolution. The above figure (right panel) shows these both for green and UV laser radiation, for lidar parameters as given above, for a laser beam diameter $2w_0$ = 50 mm, telescope diameter D = 500 mm and an required altitude resolution of 100 m. This result demonstrates how high height-resolution turbulence data may be acquired with state-of-the-art commercial components based on the OT angle-of-arrival lidar scheme described in (Zilberman & Kopeika, 2008, 2004).

While boundary layer processes may be studied in fractions of seconds, the hitherto inaccessible free atmosphere can be probed on a 1 s to 100 s timescale. Thus even higher altitudes, such as shallow Clear-Air-Turbulence (CAT) layers, may be investigated with sufficient temporal and spatial resolution which thus allows for in-depth atmospheric physics studies.

References

Andrews, L. C., & Phillips, R. L. *Laser beam propagation through random media* (2nd ed). SPIE Press, 2005.

Andrews, L. C., Phillips, R. L., Wayne, D., Sauer, P., Leclerc, T., & Crabbs, R. Creating a Cn^2 profile as a function of altitude using scintillation measurements along a slant path. In S. J. Davis, M. C. Heaven, J. T. Schriempf, & O. Korotkova (Eds.), *Proc. SPIE 8238, High Energy/Average Power Lasers and Intense Beam Applications VI; Atmospheric and Oceanic Propagation of Electromagnetic Waves VI* (p. 82380f), 2012. https://doi.org/10.1117/12.913756

Fried, D. L., & Cloud, J. D. Propagation of an Infinite Plane Wave in a Randomly Inhomogeneous Medium. *JOSA*, *56*(12), 1667–1676, 1966. https://doi.org/10.1364/JOSA.56.001667

Liu, L., Yao, Y., Vernin, J., Wang, H., Chadid, M., Wang, Y., Giordano, C., Yin, J., & Qian, X. Optical turbulence profiling with single star SCIDAR technique. *Chinese Science Bulletin*, *58*(36), 4566–4570, 2013. https://doi.org/10.1007/s11434-013-6083-9

Sathe, A., & Mann, J. A review of turbulence measurements using ground-based wind lidars. *Atmospheric Measurement Techniques*, *6*(11), 3147–3167, 2013. https://doi.org/10.5194/amt-6-3147-2013

Vaughan, J. M., Geddes, N. J., Flamant, P. H., & Flesia, C. Establishment of a backscatter coefficient and atmospheric database. *ESA-CR12510*, *22*, 1998.

Vernin, J., Chadid, M., Aristidi, E., Agabi, A., Trinquet, H., & Van der Swaelmen, M. First single star scidar measurements at Dome C, Antarctica. *Astronomy & Astrophysics*, *500*(3), 1271–1276, 2009. https://doi.org/10.1051/0004-6361/200811119

Vrancken, P., & Herbst, J. Development and Test of a Fringe-Imaging Direct-Detection Doppler Wind Lidar for Aeronautics. *EPJ Web of Conferences*. 29th International Laser Radar Conference, Hefei, People's Republic of China, 2019. https://elib.dlr.de/123605/

Zilberman, A., & Kopeika, N. S. Laser beam wander in the atmosphere: Implications for optical turbulence vertical profile sensing with imaging LIDAR. *Journal of Applied Remote Sensing*, *2*(1), 023540, 2008. https://doi.org/10.1117/1.3008058

Zilberman, A., & Kopeika, N. S. LIDAR measurements of atmospheric turbulence vertical profiles. *Free-Space Laser Communication Technologies XVI*, *5338*, 288–298, 2004. https://doi.org/10.1117/12.532386